Biosci. Biotechnol. Biochem., **68** (10), 2138–2147, 2004

Gene Cloning and Biochemical Characterizations of Thermostable Ribonuclease HIII from *Bacillus stearothermophilus*

Hyongi CHON,[1] Rikita NAKANO,[1] Naoto OHTANI,[1] Mitsuru HARUKI,[1,*] Kazufumi TAKANO,[1,2] Masaaki MORIKAWA,[1,**] and Shigenori KANAYA[1,†]

[1]*Department of Material and Life Science, Graduate School of Engineering, Osaka University, 2-1 Yamadaoka, Suita, Osaka 565-0871, Japan*

[2]*PRESTO, JST, 2-1 Yamadaoka, Suita, Osaka 565-0871, Japan*

Received May 26, 2004; Accepted July 7, 2004

The gene encoding RNase HIII from the thermophilic bacterium *Bacillus stearothermophilus* was cloned and overexpressed in *Escherichia coli*, and the recombinant protein (Bst–RNase HIII) was purified and biochemically characterized. Bst–RNase HIII is a monomeric protein with 310 amino acid residues, and shows an amino acid sequence identity of 47.1% with *B. subtilis* RNase HIII (Bsu–RNase HIII). The enzymatic properties of Bst–RNase HIII, such as pH optimum, metal ion requirement, and cleavage mode of the substrates, were similar to those of Bsu–RNase HIII. However, Bst–RNase HIII was more stable than Bsu–RNase HIII, and the temperature ($T_{1/2}$) at which the enzyme loses half of its activity upon incubation for 10 min was 55 °C for Bst–RNase HIII and 35 °C for Bsu–RNase HIII. The optimum temperature for Bst–RNase HIII activity was also shifted upward by roughly 20 °C as compared to that of Bsu–RNase HIII. The availability of such a thermostable enzyme will facilitate structural studies of RNase HIII.

Key words: ribonuclease H (RNase H); *Bacillus stearothermophilus*; stability; metal dependence; DNA/RNA hybrid

Ribonuclease H (RNase H) (EC 3.1.26.4) endonucleolytically cleaves RNA of RNA/DNA hybrids at the PO-3′ bond.[1)] The enzyme requires divalent cations, such as Mg^{2+} and Mn^{2+}, for activity. RNase H is universally present in various organisms, including bacteria, archaea, and eukaryotes.[2)] It is also present in retroviruses as a C-terminal domain of reverse transcriptase (RT). Based on differences in amino acid sequences, RNases H are classified into two major families, type 1 and type 2 RNases H, which are evolutionarily unrelated.[2)] The physiological roles of these RNases H remain to be fully understood. However, the data accumulated so far indicate that the enzyme is involved in DNA replication, repair, and/or transcription.[3–9)] The RNase H domain of RT is required for proliferation of HIV-1, and is therefore regarded as one of the targets for AIDS therapy.[10)] In antisense therapy, RNase H plays a critical role in the antisense effects of deoxyoligonucleotides.[11)]

Prokaryotic RNases H are divided into three groups, RNases HI, HII, and HIII, which are encoded by the *rnhA*, *rnhB*, and *rnhC* genes, respectively.[2,12)] RNases HI are members of the type 1 RNase H family, while RNases HII and HIII are members of the type 2 RNase H family. RNase HIII shows poor amino acid sequence identity with RNase HII. Nevertheless, RNases HII and HIII are classified into the same family, because several sequence motifs are well conserved in these sequences.[12)]

Prokaryotic RNases HI and HII have been extensively studied for structures and functions. The crystal structures of RNases HI from *E. coli*[13,14)] and *Thermus thermophilus*,[15)] and RNases HII from *Methanococcus jannaschii*,[16)] *Thermococcus kodakaraensis*,[17)] and *Archaeoglobus fulgidus*[18)] have been determined. The crystal structures of bacterial RNases HI, which highly resemble that of the RNase H domain of HIV-1 RT,[19–21)] represent type 1 RNase H structure, and those of RNases HII from hyperthermophilic archaea, which highly resemble with one another, represent type 2 RNase H structure. Comparison of these structures indicated that type 1 and type 2 RNases H share a main chain fold consisting of a five-stranded β-sheet and two α-helices.

† To whom correspondence should be addressed. Fax: +81-6-6879-7938; E-mail: kanaya@mls.eng.osaka-u.ac.jp

* Present address: *Department of Materials Chemistry and Engineering, College of Engineering, Nihon University, Tamura-machi, Koriyama, Fukushima 963-8642, Japan*

** Present address: *Laboratory of Environmental Molecular Biology, Graduate School of Environmental Earth Science, Hokkaido University, Sapporo 060-0810, Japan*

Abbreviations: RNase H, ribonuclease H; RT, reverse transcriptase; CD, circular dichroism; Bsu–RNase HIII, *B. subtilis* RNase HIII; Bst–RNase HIII, *B. stearothermophilus* RNase HIII

Steric configurations of the four acidic active-site residues are similar in these proteins, suggesting that these enzymes share a common catalytic mechanism. According to a catalytic mechanism currently proposed for *E. coli* RNase HI,[22–24] the enzyme exhibits the activity upon binding of a single metal ion and a water molecule attacking an RNA phosphate group is activated by either an amino acid or a metal ion. A similar mechanism has been proposed for RNases HII.[25] However, RNases HI and HII differ in the location of the substrate binding domain. According to docking models of the RNA/DNA hybrid on RNase HI[26] and RNase HII,[17] which are supported by the crystal structure of HIV-1 RT in complex with RNA/DNA hybrid,[27] the catalytic and substrate binding domains contact the substrate in a way such that they are located either along (RNase HI) or across (RNase HII) the helical structure of the substrate.

As compared to RNases HI and HII, much less is known about the structures and functions of RNases HIII. *B. subtilis* RNase HIII (Bsu–RNase HIII) is the only RNase HIII enzyme which has so far been analyzed for biochemical properties.[12] This enzyme is evolutionarily more distantly related to RNase HI than to RNase HII. Nevertheless, it is more closely related to RNase HI than to RNase HII in enzymatic properties, such as metal ion specificities, specific activities, and cleavage site specificities. Bsu–RNase HIII, however, is not suitable for structural studies due to its instability.

B. stearothermophilus CU21 is a thermophilic bacterium with maximum and minimum growth temperatures of 70 and 40 °C, respectively.[28] This bacterium has been shown to produce thermostable α-amylase[29] and neutral protease.[30] In this study, we cloned the *Bst–rnhC* gene encoding RNase HIII (Bst–RNase HIII) from this strain, overexpressed it in *E. coli*, purified the recombinant protein, and characterized its enzymatic properties. The enzyme was more stable than Bsu–RNase HIII, as expected, and exhibited similar enzymatic properties. The availability of such a thermostable RNase HIII might facilitate structural studies of RNase HIII.

Materials and Methods

Cells and plasmids. The thermophilic bacterium *Bacillus stearothermophilus* CU21 was previously isolated.[28] *E. coli* MIC3001 [F^-, *supE44*, *supF58*, *lacY1 or Δ(lacIZY)6*, *trpR55*, *galK2*, *galT22*, *metB1*, *hsdR14*($r_K^- m_K^+$), *rnhA339::cat*, *recB270*][31] and *E. coli* MIC2067 [F^-, λ^-, IN(*rrn*D–*rrn*E)1, *rnhA339::cat*, *rnhB716::kam*][32] were kindly donated by M. Itaya. A λDE3 lysogen of *E. coli* MIC2067, *E. coli* MIC2067(DE3), was previously constructed.[33] Plasmids pBR322 and pUC18 were obtained from Takara Shuzo (Kyoto, Japan), and pET-25b was from Novagen (Madison, WI, U.S.A). *E. coli* MIC2067(DE3) transformants were grown in NZCYM medium (Novagen) containing 50 mg/l ampicillin and 0.1% glucose. Other *E. coli* transformants were grown in Luria–Bertani medium containing 50 mg/l ampicillin.

Materials. [[γ-^{32}P]ATP (>5000 Ci/mmol) was obtained from Amersham Biosciences (Piscataway, NJ, U.S.A). *Crotalus durissus* phosphodiesterase was from Boehringer Mannheim (Tokyo, Japan). Recombinant Bsu–RNase HIII was purified as previously described.[12] All DNA oligomers for PCR were synthesized by Hokkaido System Science (Sapporo, Japan). Restriction and modifying enzymes were from Takara Shuzo.

Cloning of the Bst–rnhC gene. The genomic DNA of *B. stearothermophilus* CU21 was prepared as described previously[34] and used as a template to amplify the part of the gene (*Bst–rnhC*) encoding Bst–RNase HIII by polymerase chain reaction (PCR). The sequences of the PCR primers were 5′-GTTATCGGTTCTGACGAAG-TCGGA-3′ for the 5′-primer and 5′-CGCTTTTTGC-GTATTGGCGAAATGGAGTTT-3′ for the 3′-primer. PCR was performed with the GeneAmp PCR system 2400 (Perkin-Elmer Japan, Tokyo), using a KOD polymerase (Toyobo, Kyoto, Japan) according to the procedures recommended by the supplier. The amplified DNA fragment (630 bp) was used as a probe for Southern blotting and colony hybridization to clone the entire *Bst–rnhC* gene. Southern blotting and colony hybridization were carried out using the AlkPhos Direct system (Amersham Biosciences) according to the procedures recommended by the supplier. The DNA sequence was determined with a Prism 310 DNA sequencer (Perkin-Elmer Japan).

Plasmid construction. Plasmid pBR1300st for complementation assay of Bst–RNase HIII was constructed by performing PCR twice, as described previously for the construction of pBR800es.[12] The sequences of the PCR primers were 5′-TTCAAGAATTCTCATGTT-TTGAC-3′ for the 5′-primer, 5′-GCGGTCGACGTCC-CAAGAGAA-3′ for the 3′-primer, 5′-TCTACCA-GAGATG*TCAAACTATGT*-3′ for the 5′-fusion primer, and 5′-*AGTTTGA*CATCTCTGGTAGACTTCCTGTA-A-3′ for the 3′-fusion primer. In these sequences, underlined bases show the positions of the *Eco*RI (5′-primer) and *Sal*I (3′-primer) sites, boxed bases show the position of the codon for the initial methionine residue, and italic bases represent those of the *Bst–rnhC* gene.

Plasmid pET1000st for overproduction of Bst–RNase HIII was constructed by ligating the DNA fragment, which was amplified by PCR using the cloned *Bst–rnhC* gene as a template, into the *Nde*I–*Sal*I sites of pET-25b. The sequences of the PCR primers were 5′-AGGAG-CAGATCGACATATGTCAAACTATGT-3′ for the 5′-primer and 5′-CGCGCGGTCGACGTCCCAAGAGA-ACGGGGCACCCCTT-3′ for the 3′-primer, where underlined bases show the position of the *Nde*I (5′-primer) and *Sal*I (3′-primer) sites. Note that the initiation codon of the *Bst–rnhC* gene was changed from TTG to

ATG for construction of plasmids pBR1300st and pET1000st.

Overproduction and purification. *E. coli* MIC2067(DE3) was transformed with pET1000st, in which the transcription of the *Bst–rnhC* gene is controlled by the T7 promoter, and grown at 30 °C. When the absorbance at 660 nm of the culture reached about 0.5, 1 mM of isopropyl β-D-thiogalactopyranoside (IPTG) was added to the culture medium and cultivation was continued at 30 °C for 4 h. Cells were harvested by centrifugation at 6000 *g* for 10 min, suspended in 10 mM Tris–HCl (pH 7.5) containing 1 mM EDTA (TE buffer), disrupted by sonication lysis, and centrifuged at 30,000 *g* for 30 min. Ammonium sulfate was added to the supernatant to a concentration of 70%, and the resultant precipitates were collected by centrifugation at 15,000 *g* for 30 min. The precipitates were then dissolved in TE buffer, dialyzed against TE buffer, and loaded onto a Hitrap Heparin HP column (Amersham Biosciences) equilibrated with TE buffer. The protein was eluted from the column with a linear gradient of 0–0.5 M NaCl. The fractions containing Bst–RNase HIII were collected and loaded onto a HiLoad 16/60 Superdex 200 pg column (Amersham Biosciences) equilibrated with 20 mM sodium acetate (pH 5.0) containing 1 mM EDTA and 0.1 M NaCl. The purity of the protein was confirmed by SDS–PAGE,[35] followed by staining with Coomassie Brilliant Blue R250. The protein concentration was determined from UV absorption using an A_{280} value of 0.73 for 0.1% solution. This value was calculated by using $\varepsilon = 1576\ M^{-1}$ for Tyr and $5225\ M^{-1}$ for Trp at 280 nm.[36]

Circular dichroism (CD) spectra. The far-UV (200–260 nm) CD spectra were measured on a J-725 spectropolarimeter (Japan Spectroscopic, Tokyo, Japan) at 25 °C using a solution containing the protein at 0.1 mg/ml in 10 mM Tris–HCl (pH 7.5) containing 0.15 M NaCl in a cell with an optical path length of 2 mm. The mean residue ellipticity, θ, which has units of degrees per square centimeter per decamole, was calculated using an average amino acid molecular weight of 110.

Enzymatic activity. The RNase H activity was determined at 30 °C for 15 min by measuring the amount of radioactivity of the acid-soluble digestion product from the substrate, the ^{3}H-labeled M13 DNA–RNA hybrid, as previously described.[37] The buffer was 10 mM Tris–HCl (pH 8.5) containing 50 mM $MgCl_2$, 100 mM KCl (Bst–RNase HIII) or NaCl (Bsu–RNase HIII), 1 mM 2-mercaptoethanol (2-Me), and 50 μg/ml bovine serum albumin (BSA). One unit was defined as the amount of enzyme producing 1 μmol of acid-soluble material per min at 30 °C. Specific activity was defined as enzymatic activity per milligram of protein.

For the determination of kinetic parameters, the substrate concentration was varied from 0.10 to 1.0 μM. The amount of the enzyme was controlled in such a way that the fraction of the substrate hydrolyzed did not exceed 30% of the total. Under this condition, the amount of the product increased in proportion to increases in the reaction time. Hydrolysis of the M13 RNA/DNA hybrid by the enzyme followed Michaelis–Menten kinetics, and the kinetic parameters were determined from the Lineweaver–Burk plot. For analysis of pH dependence, 10 mM BisTris–HCl (pH 5.7–7.1), Tris–HCl (pH 7.1–8.8), or glycine–NaOH (pH 8.3–10.0) was used as a buffer for assay procedures. For analysis of divalent cation or salt dependence, enzymatic activity was determined in the presence of various concentrations of $MgCl_2$, $MnCl_2$, $CoCl_2$, $NiCl_2$, NaCl, or KCl.

Cleavage of oligomeric substrates. The 29-base pair DNA–RNA–DNA/DNA and the 12-base pair RNA/DNA duplexes (1 μM) were prepared by hybridizing the 5′-end-labeled 29-base DNA–RNA–DNA (5′-AATAG-AGAAAAAGaaaaAAGATGGCAAAG-3′) and 12-base RNA (5′-cggagaugacgg-3′) with 1.5 molar equivalent of the complementary DNAs, respectively, as previously described.[12] In these sequences, DNA and RNA are represented by uppercase and lowercase letters, respectively. Hydrolysis of the substrate at 30 °C for 15 min and separation of the products on a 20% polyacrylamide gel containing 7 M urea were carried out as previously described.[12] The reaction buffer was the same as that for the hydrolysis of the M13 DNA/RNA hybrid. The products were identified by comparing their migration on the gel with those of the oligonucleotides generated by partial digestion of 29-base DNA–RNA–DNA or 12-base RNA with snake venom phosphodiesterase.[38]

Results

Gene cloning

Comparison of the amino acid sequences of various bacterial RNases HIII indicated that the sequences VIGSDEVG and KLHFANTQKA, which correspond to Val^{96}–Gly^{103} and Lys^{295}–Ala^{304} of Bsu–RNase HIII, respectively, are highly conserved.[2] Therefore we constructed the PCR primers based on these sequences and used them to amplify the part of the *Bst–rnhC* gene that encodes Bst–RNase HIII.

PCR using the genomic DNA of *B. stearothermophilus* CU21 as a template produced a 630-bp DNA fragment that encodes a part of the Bst–RNase HIII sequence. Southern blotting and colony hybridization using this DNA fragment as a probe indicated that a 4-kbp *Sal*I fragment of the CU21 genome contained the entire *Bst–rnhC* gene (data not shown). Determination of the nucleotide sequence of the *Bst–rnhC* gene indicated that Bst–RNase HIII is composed of 310 amino acid residues with a calculated molecular weight of 33,734 and an isoelectric point (p*I*) of 8.6. A potential Shine Dalgarno (SD) sequence (AGGAG), which is complementary to the 3′-end of the *B. stearothermophi-*

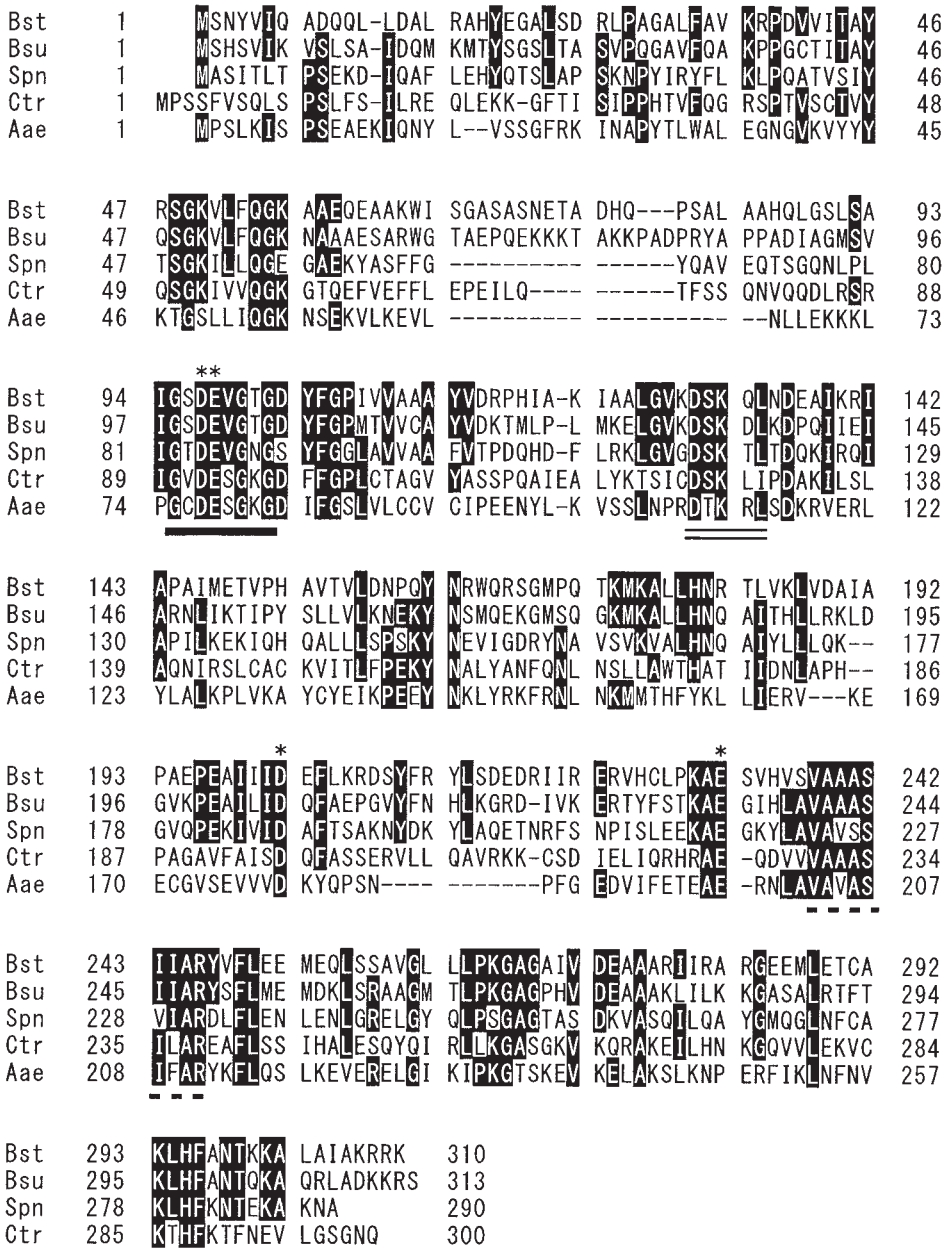

Fig. 1. Alignment of the RNase HIII Sequences.

The amino acid sequences of RNases HIII from *B. stearothermophilus* (Bst), *B. subtilis* (Bsu), *S. pneumoniae* (Spn), *C. trachomatis* (Ctr), and *A. aeolicus* (Aae) are shown. The accession nos. are Z75208 for Bsu–RNase HIII, U93576 for Spn–RNase HIII, AE001275 for Ctr–RNase HIII, and AE000755 for Aae–RNase HIII. Amino acid residues conserved in at least three different proteins are highlighted in black. Gaps are denoted by dashes. The conserved residues in various RNase HIII sequences, which are expected to form the active-site (Asp^{97}, Glu^{98}, Asp^{202}, and Glu^{232}), are denoted by asterisks (*). Three sequence motifs conserved in type 2 RNase H sequences are shown by a thick line for GXDEXGXG, a double line for DSKXL, and a broken line for VAAASIIAK below the alignments. The numbers represent the positions of the amino acid residues relative to the initiator methionine for each protein.

lus 16S rRNA sequence (accession no. M13610), is located 11 nucleotides upstream of the initiation codon TTG for translation. The nucleotide sequence of the *Bst–rnhC* gene is deposited in DDBJ under accession no. AB179782.

Amino acid sequence

The amino acid sequence of Bst–RNase HIII deduced from the nucleotide sequence is compared with those of other bacterial RNases HIII in Fig. 1. Bst–RNase HIII shows amino acid sequence identities of 47.1% with Bsu–RNase HIII, 34.8% with *Streptococcus pneumoniae* RNase HIII, 25.3% with *Chlamydia trachomatis* RNase HIII, and 22.6% with *Aquifex aeolicus* RNase HIII. According to the alignments of various type 2 RNase H sequences,[12] three sequence motifs are conserved. They are G–X–D–E–X–G–X–G, D–S–K–X–L, and V/I–A–A–A–S–I–I/L–A–K/R, where X represents any amino

acid. These sequences are well conserved in the Bst–RNase HIII sequence (Gly^{95}–Gly^{102}, Asp^{130}–Leu^{134}, and Val^{238}–Arg^{246}). In addition, four acidic active-site residues are conserved in the Bst–RNase HIII sequence. These are Asp^{97}, Glu^{98}, Asp^{202}, and Glu^{232}, which correspond to Asp^{7}, Glu^{8}, Asp^{105}, and Asp^{135} of *T. kodakaraensis* RNase HII, respectively. Note that the last residue is conserved as Asp in the RNase HII sequences, whereas it is conserved as Glu in the RNase HIII sequences.[2)]

Complementation assay

E. coli mutant strains MIC3001[31)] and MIC2067[32)] show RNase H-dependent temperature-sensitive growth phenotype. They can form colonies at 30 °C, but not at 42 °C. The temperature-sensitive growth phenotype of *E. coli* MIC3001 has been found to be complemented by type 2 RNases H.[12,39)] To examine whether the *Bst–rnhC* gene complements the temperature-sensitive growth phenotype of these strains, *E. coli* MIC3001 and MIC2067 cells were transformed with pBR1300st, in which the transcription and translation of the *Bst–rnhC* gene are under the control of the promoter and the SD sequence of the *E. coli* RNase HI gene. The resultant MIC3001 and MIC2067 transformants grew at 42 °C, suggesting that Bst–RNase HIII exhibits enzymatic activity *in vivo*.

Biochemical properties of recombinant protein

We used *E. coli* mutant strain MIC2067(DE3), which lacks all functional RNases H (RNases HI and HII), as a host for overproduction of Bst–RNase HIII to avoid contamination of host-derived RNases H. Upon induction for overproduction, the recombinant protein accumulated in a soluble form and was purified to give a single band on SDS–PAGE (Fig. 2). Its production level

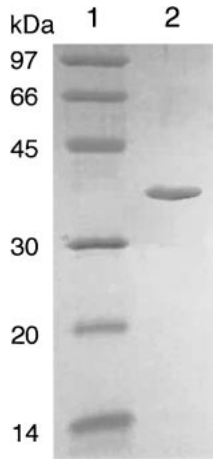

Fig. 2. SDS–PAGE of the Purified Bst–RNase HIII.

The samples were subjected to 12% SDS–PAGE and stained with Coomassie Brilliant Blue. Lane 1, a low molecular weight marker kit (Amersham Biosciences); lane 2, Bst–RNase HIII. Numbers along the gel represent the molecular masses of individual standard proteins.

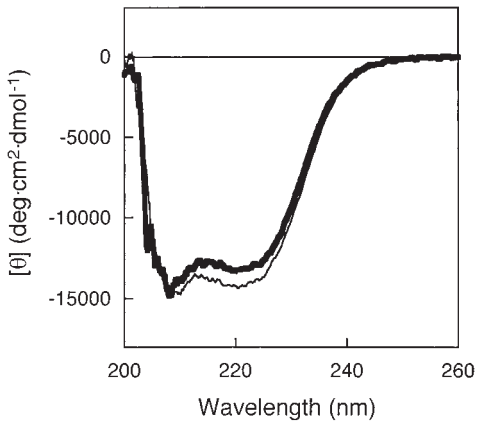

Fig. 3. CD Spectra.

The far-UV CD spectra of Bst–RNase HIII (thick line) and Bsu–RNase HIII (thin line) are shown. These spectra were measured as described in "Materials and Methods".

was estimated to be roughly 40 mg/liter culture, and approximately 10 mg of the purified protein was obtained from 1-liter culture. Purified recombinant Bst–RNase HIII and Bsu–RNase HIII are designated simply Bst–RNase HIII and Bsu–RNase HIII in this rport.

The molecular weight of Bst–RNase HIII was estimated to be 36,000 from both SDS–PAGE and gel filtration column chromatography (data not shown), indicating that Bst–RNase HIII exists in a monomeric form. The far-UV CD spectrum of Bst–RNase HIII was similar to that of Bsu–RNase HIII (Fig. 3), suggesting that its overall main chain fold is similar to that of Bsu–RNase HIII.

Enzymatic activity

The enzymatic activity of Bst–RNase HIII was determined under various conditions using the M13 DNA/RNA hybrid as a substrate. Like Bsu–RNase HIII, Bst–RNase III exhibited enzymatic activity only at an alkaline pH. The optimum pH for its activity was 8.5–9.0 (data not shown). The dependence of enzymatic activity on salt concentration was analyzed for NaCl and KCl. Like Bsu–RNase HIII, Bst–RNase HIII exhibited the highest activity in the presence of 100–200 mM salt (data not shown). However, unlike Bsu–RNase HIII, which exhibits similar activity in the presence of NaCl and KCl,[12)] Bst–RNase HIII exhibited higher activity in the presence of KCl than in that of NaCl by roughly 30%.

The dependence of Bst–RNase HIII activity on metal ion concentration was analyzed for Mg^{2+}, Mn^{2+}, Co^{2+}, and Ni^{2+} (Fig. 4). Like Bsu–RNase HIII, Bst–RNase HIII exhibited the highest activity in the presence of 50 mM $MgCl_2$. However, unlike Bsu–RNase HIII, which exhibits only 5% of maximal activity in the presence of Mn^{2+},[12)] Bst–RNase HIII exhibited roughly 60% of maximal activity in the presence of Mn^{2+}. Likewise, Bsu–RNase HIII exhibits 4.3 and 0.7% of maximal activity in the presence of Co^{2+} and Ni^{2+}, respective-

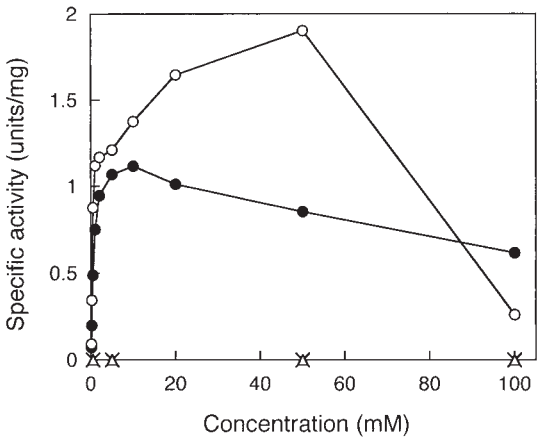

Fig. 4. Dependence of Bst–RNase HIII Activity on Divalent Metal Ion Concentrations.

The enzymatic activities of Bst–RNase HIII were determined at 30 °C in 10 mM Tris–HCl (pH 8.5) containing 100 mM KCl, 1 mM 2-mercaptoethanol, 50 μg/ml bovine serum albumin, and various concentrations of $MgCl_2$ (○), $MnCl_2$ (●), $CoCl_2$ (△), or $NiCl_2$ (×), using M13 DNA/RNA hybrid as a substrate. Note that Bst–RNase HIII showed little RNase H activity in the presence of <0.1 mM of these metal ions.

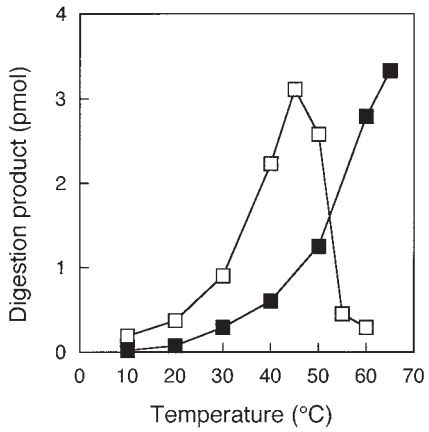

Fig. 5. Temperature Dependence of the Activities of Bst–RNase HIII and Bsu–RNase HIII.

The M13 DNA/RNA hybrid (10 pmol) was hydrolyzed by 10 pg of Bst–RNase HIII (■) or 6 pg of Bsu–RNase HIII (□) at the temperatures indicated in 10 μl of the reaction mixture for 15 min, and the amount of acid-soluble digestion products accumulated upon enzymatic reaction was plotted against the temperature. The composition of the reaction mixture for assay is described in "Materials and Methods".

Table 1. Kinetic Parameters

Enzyme	Metal ion	K_m (μM)	V_{max} (units/mg)
Bst–RNase HIII	Mg^{2+}	0.48	2.6
	Mn^{2+}	0.22	1.5
Bsu–RNase HIII	Mg^{2+}	0.25	14
	Mn^{2+}	0.17	0.7

The kinetic parameters of the enzymes were determined at 30 °C in the presence of 50 mM $MgCl_2$ or 10 mM $MnCl_2$ using the M13 RNA/DNA hybrid as a substrate, as described in "Materials and Methods". The substrate concentration was varied from 0.1 to 1.0 μM. Errors, which represent the 67% confidence limit, are all at or below ± 20% of the values reported.

Table 2. Specific Activities

Enzyme	Temperature (°C)	Specific activity (units/mg)
Bst–RNase HIII	30	1.9
	40	3.9
	50	8.2
	60	18
Bsu–RNase HIII	30	10
	40	25

The specific activities of the enzymes were determined in the presence of 50 mM $MgCl_2$ using the M13 RNA/DNA hybrid as a substrate, as described in "Materials and Methods". The substrate concentration was 1.0 μM. The reaction was carried out for 15 min at the temperatures indicated. Errors, which represent the 67% confidence limit, are all at or below ± 20% of the values reported.

ly,[12] whereas Bst–RNase HIII exhibited little activity in the presence of these divalent cations. The kinetic parameters of Bst–RNase HIII and Bsu–RNase HIII were determined at 30 °C in the presence of 50 mM $MgCl_2$ or 10 mM $MnCl_2$. The results are summarized in Table 1. The V_{max} value of Bst–RNase HIII was 5-fold lower than that of Bsu–RNase HIII when Mg^{2+} was used as a metal cofactor, whereas it was 2-fold higher than that of Bsu–RNase HIII when Mn^{2+} was used as such. The K_m values of these enzymes were comparable with one another, regardless of whether they were determined in the presence of Mg^{2+} or Mn^{2+}. These results suggest that the differences between Bst–RNase HIII and Bsu–RNase HIII activities and between their activities in the presence of Mg^{2+} and Mn^{2+} mainly reflect the difference in their hydrolysis rates, as opposed to their substrate binding affinities.

The temperature dependence of enzymatic activity was analyzed at 10–65 °C. It was not analyzed at >70 °C, because the substrate is not stable at high temperatures. As long as the amounts of acid-soluble digestion products accumulated upon 15 min incubation with the enzyme at 10–65 °C were compared with one another, Bst–RNase HIII most effectively hydrolyzed the substrate at 65 °C, whereas Bsu–RNase HIII did so at 45 °C (Fig. 5). Thus the optimum temperature for Bst–RNase HIII activity was apparently shifted upward by at least 20 °C as compared to that for Bsu–RNase HIII activity. The specific activities of Bst–RNase HIII and Bsu–RNase HIII at various temperatures are summarized in Table 2. The specific activities of Bst–RNase HIII at 60 and 50 °C were comparable to those of Bsu–RNase HIII at 40 and 30 °C, respectively, suggesting that the specific activities of these enzymes at the optimal growth temperatures of their host organisms (~65 °C for *B. stearothermophilus* and ~45 °C for *B. subtilis*) are similar. The specific activities of Bst–RNase HIII and Bsu–RNase HIII were not determined at temperatures higher than 60 and 40 °C, respectively, because the

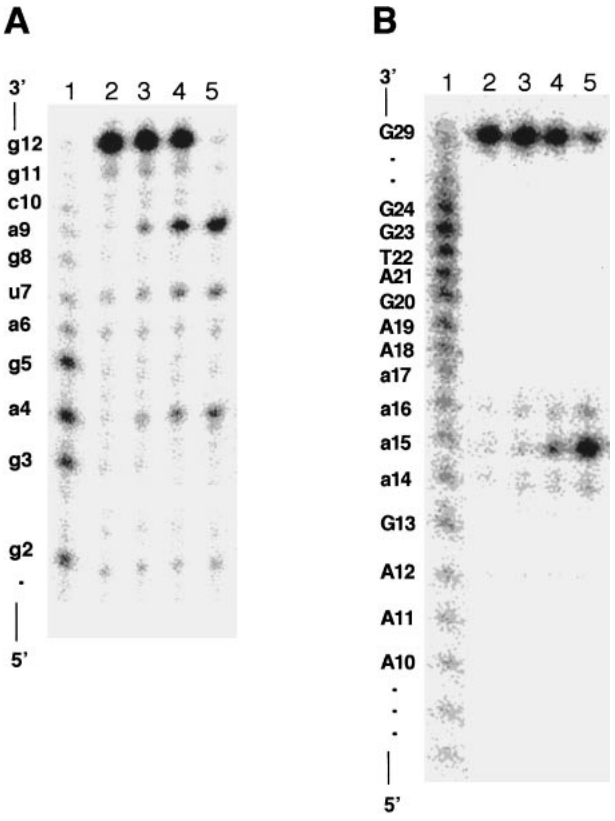

Fig. 6. Autoradiograph of Cleavage Reaction Products by Bst–RNase HIII.

Hydrolyses of the 5′-end labeled 12-base RNA hybridized to the 12-base DNA (A) and of the 5′-end labeled 29-base DNA–RNA–DNA hybridized to the 29-base DNA (B) with Bst–RNase HIII were carried out at 30 °C for 15 min. Products were separated on a 20% polyacrylamide gel containing 7 M urea, as described in "Materials and Methods". The concentration of the substrate was 1.0 μM. (A) Lane 1, partial digest of the 12-base RNA with snake venom phosphodiesterase; lane 2, untreated substrate; lane 3, hydrolysate with 2.6 ng of the enzyme; lane 4, hydrolysate with 26 ng of the enzyme; lane 5, hydrolysate with 260 ng of the enzyme. (B) Lane 1, partial digest of the 29-base DNA–RNA–DNA with snake venom phosphodiesterase; lane 2, untreated substrate; lane 3, hydrolysate with 2.6 ng of the enzyme; lane 4, hydrolysate with 26 ng of the enzyme; lane 5, hydrolysate with 260 ng of the enzyme. The 3′-terminal residue of each oligonucleotide generated by partial digestion with snake venom phosphodiesterase is shown along the gel.

amounts of acid-soluble digestion products did not increase in proportion to increases in reaction time for 15 min at these temperatures. These enzymes probably are not fully stable for 15 min at these temperatures.

Cleavage of oligomeric substrates

Two different oligomeric substrates have been examined for cleavage by Bsu–RNase HIII.[12] One is a 12-base pair RNA/DNA hybrid that is cleaved at multiple sites, but most preferably at a4–g5 and less preferably at a9–c10 and c1–g2. The second is a 29-base pair DNA–RNA–DNA/DNA substrate that is cleaved mainly in the middle of the tetraribonucleotide. We used these substrates, labeled at their 5′-ends, to examine whether

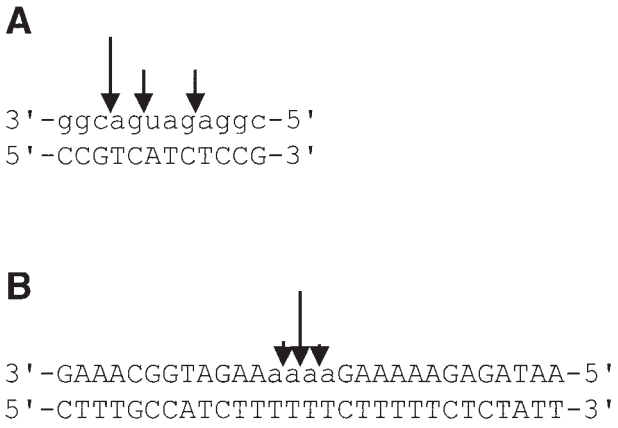

Fig. 7. Sites and Extent of Cleavages by Bst–RNase HIII.

Cleavage sites of the 12-base pair RNA/DNA hybrid (A) and those of the 29-base pair DNA–RNA–DNA/DNA substrate (B) with Bst–RNase HIII are shown by *arrows*. The differences in the lengths of the *arrows* reflect relative cleavage intensities at positions indicated. Deoxyribonucleotides are shown by *capital letters* and ribonucleotides by *small letters*.

and how Bst–RNase HIII hydrolyzes them. The results are shown in Fig. 6 and summarized in Fig. 7. When the 12-base pair RNA/DNA hybrid was used as a substrate, the enzyme cleaved it at multiple sites, as did Bsu–RNase HIII, but with a slightly different preference. It cleaved this substrate preferentially at a9–c10, with minor products resulting from cleavages at a4–g5 and u7–g8. When the 29-base pair DNA–RNA–DNA/DNA substrate was used as a substrate, Bst–RNase HIII preferentially cleaved it at the middle of the tetra-adenosine region (a15–a16), like Bsu–RNase HIII. It cleaved this substrate at a14–a15 and a16–a17 as well, but with much lower frequencies.

Stability

In order to compare the thermal stability of Bst–RNase HIII and Bsu–RNase HIII, they were incubated in 20 mM Tris–HCl (pH 7.5) containing 0.1 M NaCl, 1 mM EDTA, 10% glycerol, and 0.1 mg/ml BSA at various temperatures for 10 min, and the residual activities were determined at 30 °C. Under this condition, both enzymes were irreversible in thermal denaturation. The protein concentrations were 5–8 ng/ml. Under this condition, the temperature ($T_{1/2}$) at which the enzyme loses half of its activity was roughly 55 °C for Bst–RNase HIII and 35 °C for Bsu–RNase HIII (Fig. 8). Thus Bst–RNase HIII was more stable than Bsu–RNase HIII by roughly 20 °C in $T_{1/2}$.

Note that Bsu–RNase HIII was not fully stable at 30 °C under the condition mentioned above and that it loses roughly 20% of its activity upon incubation at 30 °C for 10 min (Fig. 8). However, when its activity was measured at 30 °C, the amount of the product increased in proportion to the reaction time for up to 30 min (data not shown). The enzyme is probably stabilized in the presence of divalent metal ions and/or substrate, such that it is fully stable at 30 °C.

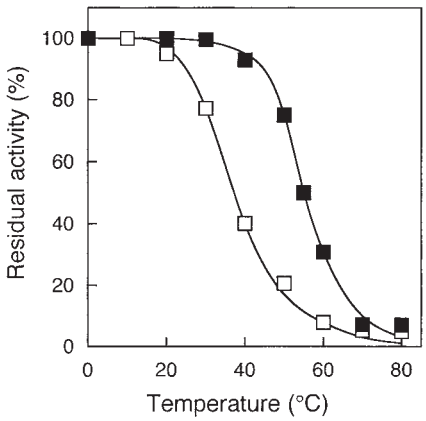

Fig. 8. Thermal Stability of Bst–RNase HIII and Bsu–RNase HIII.
The enzyme (5–8 ng/ml) was incubated in 20 mM Tris–HCl (pH 7.5) containing 0.1 M NaCl, 1 mM EDTA, 10% glycerol, and 0.1 mg/ml BSA for 10 min at the temperatures indicated and examined for residual activity at 30 °C. The residual activities of Bst–RNase HIII (■) and Bsu–RNase HIII (□) are plotted against the temperature.

Discussion

Metal ion dependence of activity

Bst–RNase HIII prefers Mg^{2+} to Mn^{2+} for activity, like Bsu–RNase HIII[12] and *E. coli* RNase HI,[23] although it shows much weaker preference for Mg^{2+} than the other two enzymes. The dependence of its activity on metal ion concentration is similar to that of Bsu–RNase HIII,[12] however, but is different from that of *E. coli* RNase HI.[23,24] Bst–RNase HIII and Bsu–RNase HIII exhibit maximal Mg^{2+}- and Mn^{2+}-dependent activities in the presence of 50 mM $MgCl_2$ and 10 mM $MnCl_2$, respectively, while *E. coli* RNase HI exhibits maximal Mg^{2+}- and Mn^{2+}-dependent activities at ~5 mM and 0.5 μM, respectively. It has been reported that the binding affinity of Mn^{2+} to *E. coli* RNase HI is higher than that of Mg^{2+} by ~100-fold, and that this difference accounts for the difference in the concentrations of these metal ions required for maximal activity.[24] Therefore Mg^{2+} and Mn^{2+} bind to Bst–RNase HIII with similar binding affinities, comparable to that of Mg^{2+} to *E. coli* RNase HI.

Crystallographic studies of *E. coli* RNase HI[40] and the RNase H domain of HIV-1 RT[19] in complex with Mn^{2+} indicated that two Mn^{2+} ions bind to the active site of the enzyme, which is formed by four acidic active-site residues. Site 1 is formed by three of them (Asp^{10}, Glu^{48}, and Asp^{70} for *E. coli* RNase HI), and site 2 is formed by two of them (Asp^{10} and Asp^{134} for *E. coli* RNase HI). These sites are located 4 Å apart. It has been proposed that *E. coli* RNase HI is activated upon binding of the first metal ion at site 1 and that this activity is attenuated upon binding of the second metal ion at site 2.[23] However, only a single Mg^{2+} ion binds to *E. coli* RNase HI at a site close to site 1 even in the presence of 50 mM $MgCl_2$,[41] suggesting that this concentration is not sufficient to allow Mg^{2+} to bind site 2. The dissociation constant of the first Mg^{2+} ion has been found to be 200 μM[42] or 710 μM.[43] The dissociation constant of the second Mg^{2+} ion might increase dramatically due to a dramatic decrease in the negative charge density at the active site upon binding of the first Mg^{2+} ion.

The similarity in the configurations of the four acidic active-site residues, which are fully conserved in the RNase H sequences, in type 1 and type 2 RNase H structures[16–18] might suggest that the two metal binding sites identified in the *E. coli* RNase HI structure are conserved in all RNase H structures. In fact, the activities of *E. coli* RNase HII,[33] *A. fulgidus* RNase HII,[44] and Bsu–RNase HII[12] are also strongly attenuated at high metal ion concentrations. However, attenuation of activity at high metal ion concentrations was not clearly detected for the Mg^{2+}- or Mn^{2+}-dependent activity of Bst–RNase HIII either (Fig. 4). Mg^{2+} has a high concentration inhibition profile similar to that of *E. coli* RNase HI (Fig. 4). However, it is unclear whether this is caused by binding of the second Mg^{2+} ion at site 2, because Mg^{2+} interacts strongly with the substrate and thereby inhibits activity at high concentrations. It has also been reported with respect to Bsu–RNase HIII,[12] *M. jannaschii* RNase HII,[25] and *T. kodakaraensis* RNase HII[39] that neither Mg^{2+} nor Mn^{2+} has a high concentration inhibition profile. The second Mg^{2+} or Mn^{2+} ion might not be able to bind site 2 of these enzymes due to their weak binding affinities. Alternatively, these enzymes contain only a single metal binding site.

Multiplicity of the RNase H genes

Single bacterial and eukaryotic genomes usually contain two different genes encoding type 1 and type 2 RNases H.[2] For example, the *E. coli* genome contains the RNase HI and RNase HII genes, and the human genome contains the RNase H1 and RNase H2 genes. The *B. subtilis* genome also contains two RNase H genes, but is unique in the combination of the types of RNases H. It contains two type 2 RNase H genes, *viz.*, the RNase HII and RNase HIII genes. Previously we found that the *B. stearothermophilus* genome contains the RNase HII gene,[45] indicating that this genome also contains the RNase HII and RNase HIII genes.

The physiological significance of the multiplicity of the RNase H genes in single cells remains to be understood. However, a *B. subtilis* mutant lacking both the RNase HII gene and the RNase HIII gene exhibits a lethal growth phenotype, whereas a *B. subtilis* mutant lacking either one of these genes grows normally.[32] This result suggests that these RNases H are involved in important cellular processes in a complementary manner. The combination of types of RNases H varies for different organisms.[2] However, no genome with the combination of the RNase HI and RNase HIII genes has so far been identified. The enzymatic properties of Bst–RNase HIII and Bsu–RNase HIII resemble those of

E. coli RNase HI, as opposed to those of Bst–RNase HII or Bu–RNase HII, in the metal-ion preference and cleavage site specificity of the 29-base pair DNA–RNA–DNA/DNA substrate. Hence, it is plausible to speculate that the cells require both RNase HI-like and RNase HII-like activities for normal growth. To answer the question whether RNase HIII acquires RNase HI-like activity by assuming a structure different from that of RNase HII, structural studies of RNase HIII are necessary. The availability of a thermostable *B. stearothermophilus* RNase HIII should facilitate these structural studies.

Acknowledgments

We thank Dr. M. Itaya for providing *rnh* mutant strains of *E. coli*, MIC3001, MIC3037, and MIC2067. This work was supported in part by Grants-in-Aid for National Project on Protein Structure and Functional Analyses and for Scientific Research (no. 16041229) from the Ministry of Education, Culture, Sports, Science, and Technology of Japan.

References

1) Crouch, R. J., and Dirksen, M.-L., Ribonuclease H. In "Nuclease", eds. Linn, S. M., and Roberts, R. J., Cold Spring Harbor Laboratory, Cold Spring Harbor, New York, pp. 211–241 (1982).
2) Ohtani, N., Haruki, M., Morikawa, M., and Kanaya, S., Molecular diversities of RNases H. *J. Biosci. Bioeng.*, **88**, 12–19 (1999).
3) Kogoma, T., and Foster, P. L., Physiological functions of *E. coli* RNase HI. In "Ribonucleases H", eds. Crouch, R. J., and Toulme, J. J., INSERM, Paris, pp. 39–66 (1998).
4) Murante, R. S., Henricksen, L. A., and Bambara, R. A., Junction ribonuclease: an activity in Okazaki fragment processing. *Proc. Natl. Acad. Sci. U.S.A.*, **95**, 2244–2249 (1998).
5) Qiu, J., Qian, Y., Frank, P., Wintersberger, U., and Shen, B., *Saccharomyces cerevisiae* RNase H(35) functions in RNA primer removal during lagging-strand DNA synthesis, most efficiently in cooperation with Rad27 nuclease. *Mol. Cell. Biol.*, **19**, 8361–8371 (1999).
6) Arudchandran, A., Cerritelli, S., Narimatsu, S., Itaya, M., Shin, D. Y., Shimada, Y., and Crouch, R. J., The absence of ribonuclease H1 or H2 alters the sensitivity of *Saccharomyces cerevisiae* to hydroxyurea, caffeine and ethyl methanesulphonate: implications for roles of RNases H in DNA replication and repair. *Genes Cells.*, **5**, 789–802 (2000).
7) Haruki, M., Tsunaka, Y., Morikawa, M., and Kanaya, S., Cleavage of a DNA–RNA–DNA/DNA chimeric substrate containing a single ribonucleotide at the DNA–RNA junction with prokaryotic RNases HII. *FEBS Lett.*, **531**, 204–208 (2002).
8) Sato, A., Kanai, A., Itaya, M., and Tomita, M., Cooperative regulation for Okazaki fragment processing by RNase HII and FEN-1 purified from a hyperthermophilic archaeon, *Pyrococcus furiosus. Biochem. Biophys. Res. Commun.*, **309**, 247–252 (2003).
9) Rydberg, B., and Game, J., Excision of misincorporated ribonucleotides in DNA by RNase H (type 2) and FEN-1 in cell-free extracts. *Proc. Natl. Acad. Sci. U.S.A.*, **99**, 16654–16659 (2002).
10) Nanni, R. G., Ding, J., Jacobo-Molina, A., Hughes, S. H., and Arnold, E., Review of HIV-1 reverse transcriptase three-dimensional structure: implications for drug design. *Perspectives in Drug Discovery and Design*, **1**, 129–150 (1993).
11) Toulme, J. J., and Tidd, D., Role of ribonuclease H in antisense oligonucleotide-mediated effects. In "Ribonucleases H", eds. Crouch, R. J., and Toulme, J. J., INSERM, Paris, pp. 225–250 (1998).
12) Ohtani, N., Haruki, M., Morikawa, M., Crouch, R. J., Itaya, M., and Kanaya, S., Identification of the genes encoding Mn^{2+}-dependent RNase HII and Mg^{2+}-dependent RNase HIII from *Bacillus subtilis*: Classification of RNases H into three families. *Biochemistry*, **38**, 605–618 (1999).
13) Katayanagi, K., Miyagawa, M., Matsushima, M., Ishikawa, M., Kanaya, S., Ikehara, M., Matsuzaki, T., and Morikawa, K., Three-dimensional structure of ribonuclease H from *E. coli*. *Nature*, **347**, 306–309 (1990).
14) Yang, W., Hendrickson, W. A., Crouch, R. J., and Satow, Y., Structure of ribonuclease H phased at 2 Å resolution by MAD analysis of the selenomethionyl protein. *Science*, **249**, 1398–1405 (1990).
15) Ishikawa, K., Okumura, M., Katayanagi, K., Kimura, S., Kanaya, S., Nakamura, H., and Morikawa, K., Crystal structure of ribonuclease HI from *Thermus thermophilus* HB8 refined at 2.8 Å resolution. *J. Mol. Biol.*, **230**, 529–542 (1993).
16) Lai, L., Yokota, H., Hung, L. W., Kim, R., and Kim, S. H., Crystal structure of archaeal RNase HII: a homologue of human major RNase H. *Structure*, **8**, 897–904 (2000).
17) Muroya, A., Tsuchiya, D., Ishikawa, M., Haruki, M., Morikawa, M., Kanaya, S., and Morikawa, K., Catalytic center of an archaeal Type 2 Ribonuclease H as revealed by X-ray crystallographic and mutational analyses. *Protein Sci.*, **10**, 707–714 (2001).
18) Chapados, B. R., Chai, Q., Hosfield, D. J., Shen, B., and Tainer, J. A., Structural biochemistry of a type 2 RNase H: RNA primer recognition and removal during DNA replication. *J. Mol. Biol.*, **307**, 541–556 (2001).
19) Davies, J. F. D., Hostomska, Z., Hostomsky, Z., Jordan, S. R., and Matthews, D. A., Crystal structure of the ribonuclease H domain of HIV-1 reverse transcriptase. *Science*, **252**, 88–95 (1991).
20) Kohlstaedt, L. A., Wang, J., Friedman, J. M., Rice, P. A., and Steitz, T. A., Crystal structure at 3.5 Å resolution of HIV-1 reverse transcriptase complexed with an inhibitor. *Science*, **256**, 1783–1790 (1992).
21) Jacobo-Molina, A., Ding, J., Nanni, R. G., Clark, A. D. Jr., Lu, X., Tantillo, C., Williams, R. L., Kamer, G., Ferris, A. L., Clark, P., Hizi, A., Hughes, S. H., and Arnold, E., Crystal structure of human immunodeficiency virus type 1 reverse transcriptase complexed with double-stranded DNA at 3.0 Å resolution shows bent DNA. *Proc. Natl. Acad. Sci. U.S.A.*, **90**, 6320–6324 (1993).
22) Kanaya, S., Enzymatic activity and protein stability of

E. coli ribonuclease HI. In "Ribonucleases H", eds. Crouch, R. J., and Toulme, J. J., INSERM, Paris, pp. 1–38 (1998).

23) Keck, J. L., Goedken, E. R., and Marqusee, S., Activation/attenuation model for RNase H. A one-metal mechanism with second-metal inhibition. *J. Biol. Chem.*, **273**, 34128–34133 (1998).

24) Tsunaka, Y., Haruki, M., Morikawa, M., Oobatake, M., and Kanaya, S., Dispensability of Glu^{48} and Asp^{134} for Mn^{2+}-dependent activity of *E. coli* ribonuclease HI. *Biochemistry*, **42**, 3366–3374 (2003).

25) Lai, B., Li, Y., Cao, A., and Lai, L., Metal ion binding and enzymatic mechanism of *Methanococcus jannaschii* RNase HII. *Biochemistry*, **42**, 785–791 (2003).

26) Nakamura, H., Oda, Y., Iwai, S., Inoue, H., Ohtsuka, E., Kanaya, S., Kimura, S., Katsuda, C., Katayanagi, K., Morikawa, K., Miyashiro, H., and Ikehara, M., How does ribonuclease H recognize a DNA–RNA hybrid? *Proc. Natl. Acad. Sci. U.S.A.*, **88**, 11535–11539 (1991).

27) Sarafianos, S. G., Das, K., Tantillo, C., Clark, A. D. Jr., Ding, J., Whitcomb, J. M., Boyer, P. L., Hughes, S. H., and Arnold, E., Crystal structure of HIV-1 reverse transcriptase in complex with a polypurine tract RNA:DNA. *EMBO J.*, **20**, 1449–1461 (2001).

28) Imanaka, T., Fujii, M., Aramori, I., and Aiba, S., Transformation of *Bacillus stearothermophilus* with plasmid DNA and characterization of shuttle vector plasmids between *Bacillus stearothermophilus* and *Bacillus subtilis*. *J. Bacteriol.*, **149**, 824–830 (1982).

29) Aiba, S., Kitai, K., and Imanaka, T., Cloning and expression of thermostable α-amylase gene from *Bacillus stearothermophilus* in *Bacillus stearothermophilus* and *Bacillus subtilis*. *Appl. Environ. Microbiol.*, **46**, 1059–1065 (1983).

30) Fujii, M., Takagi, M., Imanaka, T., and Aiba, S., Molecular cloning of a thermostable neutral protease gene from *Bacillus stearothermophilus* in a vector plasmid and its expression in *Bacillus stearothermophilus* and *Bacillus subtilis*. *J. Bacteriol.*, **154**, 831–837 (1983).

31) Itaya, M., and Crouch, R. J., A combination of RNase H (*rnh*) and *recBCD* or *sbcB* mutations in *Escherichia coli* K12 adversely affects growth. *Mol. Gen. Genet.*, **227**, 424–432 (1991).

32) Itaya, M., Omori, A., Kanaya, S., Crouch, R. J., Tanaka, T., and Kondo, K., Isolation of RNase H genes that are essential for growth of *Bacillus subtilis* 168. *J. Bacteriol.*, **181**, 2118–2123 (1999).

33) Ohtani, N., Haruki, M., Muroya, A., Morikawa, M., and Kanaya, S., Characterization of ribonuclease HII from *Escherichia coli* overproduced in a soluble form. *J. Biochem. (Tokyo)*, **127**, 895–899 (2000).

34) Imanaka, T., Tanaka, T., Tsunekawa, H., and Aiba, S., Cloning of the genes for penicillinase, *penP* and *penI*, of *Bacillus licheniformis* in some vector plasmids and their expression in *Escherichia coli*, *Bacillus subtilis*, and *Bacillus licheniformis*. *J. Bacteriol.*, **147**, 776–786 (1981).

35) Laemmli, U. K., Cleavage of structural proteins during the assembly of the head of bacteriophage T4. *Nature*, **227**, 680–685 (1970).

36) Goodwin, T. W., and Morton, R. A., The spectrophotometric determination of tyrosine and tryptophan in proteins. *Biochem. J.*, **40**, 628–632 (1946).

37) Kanaya, S., Katsuda, C., Kimura, S., Nakai, T., Kitakuni, E., Nakamura, H., Katayanagi, K., Morikawa, K., and Ikehara, M., Stabilization of *Escherichia coli* ribonuclease H by introduction of an artificial disulfide bond. *J. Biol. Chem.*, **266**, 6038–6044 (1991).

38) Jay, E., Bambara, R., Padmanabham, P., and Wu, R., DNA sequence analysis: a general, simple and rapid method for sequencing large oligodeoxyribonucleotide fragments by mapping. *Nucleic Acids Res.*, **1**, 331–353 (1974).

39) Haruki, M., Hayashi, K., Kochi, T., Muroya, A., Koga, Y., Morikawa, M., Imanaka, T., and Kanaya, S., Gene cloning and characterization of recombinant ribonuclease HII from a hyperthermophilic archaeon. *J. Bacteriol.*, **180**, 6207–6214 (1998).

40) Goedken, E. R., and Marqusee, S., Co-crystal of *Escherichia coli* RNase HI with Mn^{2+} ions reveals two divalent metals bound in the active site. *J. Biol. Chem.*, **276**, 7266–7271 (2001).

41) Katayanagi, K., Okumura, M., and Morikawa, K., Crystal structure of *Escherichia coli* RNase HI in complex with Mg^{2+} at 2.8 Å resolution: Proof for a single Mg^{2+}-binding site. *Proteins: Struct. Funct. Genet.*, **17**, 337–346 (1993).

42) Huang, H. W., and Cowan, J. A., Metallobiochemistry of the magnesium ion: Characterization of the essential metal-binding site in *Escherichia coli* ribonuclease H. *Eur. J. Biochem.*, **219**, 253–260 (1994).

43) Kanaya, S., Oobatake, M., and Liu, Y.-Y., Thermal stability of *E. coli* ribonuclease HI and its active-site mutants in the presence and absence of the Mg^{2+} ion: proposal of a novel catalytic role for Glu^{48}. *J. Biol. Chem.*, **271**, 32729–32736 (1996).

44) Chai, Q., Qiu, J., Chapados, B. R., and Shen, B., *Archaeoglobus fulgidus* RNase HII in DNA replication: enzymological functions and activity regulation *via* metal cofactors. *Biochem. Biophys. Res. Commun.*, **286**, 1073–1081 (2001).

45) Muroya, A., Nakano, R., Ohtani, N., Haruki, M., Morikawa, M., and Kanaya, S., Importance of an N-terminal extension of ribonuclease HII from *Bacillus stearothermophilus* for substrate binding. *J. Biosci. Bioeng.*, **93**, 170–175 (2002).